2010

A Potent and Selective Inhibitor of Cdc42 GTPase

Zurab Surviladze
University of New Mexico

Anna Waller
University of New Mexico

J. Jacob Strouse
University of New Mexico

Cristian G. Bologa
University of New Mexico

Oleg Ursu
University of New Mexico

See next page for additional authors

MolecularLibraries
Pathways to Discovery

Probe Report

Title: A Potent and Selective Inhibitor of Cdc42 GTPase

Authors: UNM Center for Molecular Discovery: Zurab Surviladze, Anna Waller, J. Jacob Strouse, Cristian Bologa, Oleg Ursu, Virginia Salas, John F. Parkinson, Genevieve K. Phillips, Elsa Romero, Angela Wandinger-Ness and Larry A. Sklar**.** Kansas University Specialized Chemistry Center: Chad Schroeder, Denise Simpson, Julica Nöth, Jenna Wang, Jennifer Golden, and Jeffrey Aubé.

Assigned Assay Grant #: MH081231-01

Screening Center Name & PI: UNM Center for Molecular Discovery, Larry Sklar
Chemistry Center Name & PI: University of Kansas, Jeffrey Aubé
Assay Submitter & Institution: Angela Wandinger-Ness, UNM

PubChem Summary Bioassay Identifier (AID): 1772
PubChem CID: 2950007
Chemical IUPAC Name: 4-[3-(4-methoxyphenyl)-5-phenyl-3,4-dihydropyrazol-2-yl]benzenesulfonamide [ML 141]

Probe Structure & Characteristics:

Molecular Weight	407.48544 [g/mol]
Molecular Formula	$C_{22}H_{21}N_3O_3S$
XLogP3-AA	3.6
H-Bond Donor	1
H-Bond Acceptor	6
Rotatable Bond Count	5
Exact Mass	407.130362
MonoIsotopic Mass	407.130362
Topological Polar Surface Area	85
Heavy Atom Count	29
Formal Charge	0
Complexity	668
Isotope Atom Count	0
Defined Atom StereoCenter Count	0
Undefined Atom StereoCenter Count	1
Defined Bond StereoCenter Count	0
Undefined Bond StereoCenter Count	0
Covalently-Bonded Unit Count	1

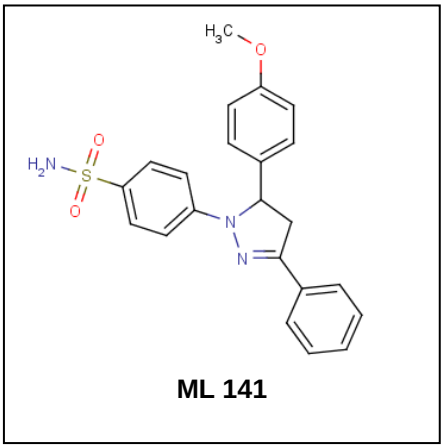

ML 141

Table 1. Profile of the Chemical Probe CID2950007 on Ras-Related GTPases

CID/ ML#**	Target Name‡	IC50/EC50 (μM)	Anti-target Name(s)‡	IC50/EC50 (μM)	Selectivity *	Assay Name and/or AIDs
2950007/ 141	Nucleotide-depleted Cdc42 wild type with 1 nM GTP and 1 mM Mg^{2+}	0.2	Glutathione S –transferase	n.d	n.d.	AID 2376
2950007/ 141	Cdc42 wild type	2.6	Glutathione S –transferase	>100	>50	AID 1758, 1762, 761, 1333, 1334, 1772, 2009, 2019, 2020, 2021, 2022, 2037, 2372, 2373, 2374, 2375, 2376, 2378, 2418
2950007/ 141	Cdc42 activated mutant	5.4	Glutathione S –transferase	>100	>50	AID 1758, 1762, 761, 1333, 1334, 1772S, 2009, 2019, 2020, 2021, 2022, 2037
2950007/ 141	Ras wild type	>100	Glutathione S –transferase	>100	Not relevant	AID 759, 1759, 1761, 1335, 2038, 2047, 2053, 1772
2950007/ 141	Ras activated mutant	>100	Glutathione S –transferase	>100	Not relevant	AID 1341
2950007/ 141	Rab 7 wild type	>100	Glutathione S –transferase	>100	Not relevant	AID 758, 1760, 1336, 2031, 204, 1772
2950007/ 141	Rab 2a wild type	>100	Glutathione S –transferase	>100	Not relevant	AID 1763, 760, 1337, 2033, 2045, 2046, 1772
2950007/ 141	Rac1 activated mutant	>100	Glutathione S –transferase	>100	Not relevant	AID 764, 1339, 2039, 2048, 2051, 1772
2950007/ 141	Rac 1 wild type	>100	Glutathione S –transferase	>100	Not relevant	AID 757, 1769, 1340,1772, 2027, 2040, 2055, 1772
2950007/ 141	Cdc42 wild type	2	n.d.	n.d.	n.d.	primary assay with 1 mM Mg^{2+} AID 2393
2950007/ 141	Cdc42 wild type	< 10	n.d.	n.d.	n.d.	GTP binding with 1 mM EDTA AID 2378
2950007/ 141	Cdc42 wild type	< 10	n.d.	n.d.	n.d.	GTP binding with Mg2+ AID 2373
2950007/ 141	Nucleotide-depleted Cdc42 wild type	< 10	n.d.	n.d.	n.d.	GTP binding with Mg^{2+} AID 2372
2950007/ 141	Cdc42-PAK-PBD complex	< 10	n.d.	n.d.	n.d.	Pull down assay 2374
2950007/ 141	Cdc42	< 10	n.d.	n.d.	n.d.	Active cdc42 GLISA in 3T3 cells + EGF AID 2375
2950007/ 141	Rac1	> 10	n.d.	n.d.	n.d.	Active Rac1 GLISA in 3T3 cells s+ EGF AID 2375
2950007/ 141	Cdc42	< 10	n.d.	n.d.	n.d.	Filopodia formation in 3T3 cells + bradykinin AID 2418

Recommendations for the scientific use of this probe and prior art overview:

The probe is a potent, selective and reversible non-competitive inhibitor of Cdc42 GTPase suitable for in vitro assays. In the most relevant secondary biochemical assay using nucleotide-depleted wild type Cdc42 in the presence of Mg^{2+} and 1 nM GTP (AID 2376), CID2950007 had an IC_{50} ~ 200 nM, an acceptable probe potency within MLPCN guidelines. In the primary HTS bead-based assay using 1 mM EDTA and 100 nM BODIPY-FL-GTP, potency for CID2950007 was IC_{50} = 2.6 and 5.4 μM for Cdc42 wild type and activated mutant, respectively. No appreciable inhibitory activity up to 100 μM was observed with Rac1, Rab2, Rab7 or Ras in the multiplex screen. The Cdc42-selective probe has low (1-10) micromolar activity in qualitative and semi-quantitative cell-based assays such as GLISA assay for active GTP-bound Cdc42/PAK-PBD complex and Cdc42-dependent function in filopodia formation in 3T3 cells. The probe appears broadly specific since it has been tested in 263 MLPCN assays with only 1 confirmed IC_{50} (2.8 μM) in a *T. cruzi* parasite replication assay in 3T3 cells that is likely Cdc42-dependent (AID 2044). As stated in the CPDP for this project there was no prior art describing direct Cdc42 inhibitors, so the discoveries reported here are highly innovative and impactful.

The function of the Rho family GTPases (Rac, Rho, and Cdc42) are known to be highly complementary if not overlapping. These include roles in cell adhesion, cytoskeletal arrangement, phagocytosis and host-pathogen interactions, motility and migration, membrane protein traffic, etc. These functions are likely to be usefully measured in human leukocytes such as neutrophils and selected leukocyte cell lines. Cdc42 selective inhibitors such as those reported here should help untangle the roles of the proteins in this family. This has proven difficult with protein knockdowns because of the potential compensation in expression of other family members. For these reasons, the identification of secramine, a molecule that inhibits membrane traffic out of the Golgi apparatus was viewed as a breakthrough. The indirect and non-selective Cdc42 inhibitor secramine was synthesized predicated on brefeldin A, which is a fungal metabolite. Secramijne was reported to work by inhibiting "activation of the Rho GTPase Cdc42, a protein involved in membrane traffic, by a mechanism dependent upon the guanine dissociation inhibitor RhoGDI. RhoGDI binds Cdc42 and antagonizes its membrane association, nucleotide exchange and effector binding. In vitro, secramine inhibits Cdc42 binding to membranes, GTP and effectors in a RhoGDI-dependent manner. In cells, secramine mimics the effects of dominant-negative Cdc42 expression on protein export from the Golgi and on Golgi polarization in migrating cells. RhoGDI-dependent Cdc42 inhibition by secramine illustrates a new way to inhibit Rho GTPases with small molecules and provides a new means to study Cdc42, RhoGDI and the cellular processes they mediate" (Pelish, 2006)

1. Scientific Rationale for Project

Rho-family GTPases and their effector proteins are major regulators of signaling pathways that control diverse biological processes. The most extensively characterized Rho-family members are RhoA, Rac1 and Cdc42 (Bishop, 2000). Actin cytoskeleton reorganization is a well characterized function for Rho GTPases: Rac1, Cdc42 and RhoA regulate lamellipodia, filopodia and stress fiber formation, respectively (Bishop, 2000). Rho-family GTPases also regulate cell-cycle progression, cell growth and survival, gene transcription, adhesion, migration, phagocytosis and cytokinesis as well as neurite extension and retraction, cellular morphogenesis and polarization (Chimini, 2000; Etienne-Manneville, 2002; Raftopoulou, 2004). Rho GTPases function as molecular switches by cycling between inactive/GDP-bound and active/GTP-bound states (Jaffe, 2005). Cycling between these states is controlled by cellular proteins such as GDP-dissociation-inhibitors (GDI), guanine nucleotide exchange factors (GEFs) and GTPase-activating proteins (GAP). Rho GTPases exist in cells predominantly in the inactive GDP-bound form associated with GDIs. By binding to the C-terminal tail of GTPases, GDIs prevent GTPases from binding to the plasma membranes and keep GTPases in the cytoplasm (Johnson, 2009; Ridley, 2006). GEFs promote GDP exchange with GTP and activate GTPases whereas GAPs stimulate GTP hydrolysis to GDP, thus inactivating GTPases (Rossman, 2005; Bos, 2007).

The function of Rho-family GTPases in disease pathogenesis has been reviewed extensively (Takai, 2001; Rossman, 2005; Van Hennik, 2005; Boettner, 2002; Gomez del Pulgar, 2005; Sahai, 2002; Vega, 2008). Identifying small, cell permeable molecules that selectively and reversibly regulate Rho GTPases is of high scientific and potentially therapeutic interest. There has been limited success in identifying inhibitors that specifically interact with small Rho family GTPases. Recently a couple of low molecular weight inhibitors for Rac1 were described (Gao, 2004; Shutes, 2007). NSC23766 is cell-permeable and directly binds to a groove of Rac1 that is critical for GEF interaction. Therefore, NSC23766 blocks Rac activation by some, but not other, GEFs that activate Rac1 (Gao, 2004). More promising is the Rac-specific inhibitor EHT1864 which binds tightly to Rac1, Rac1b, Rac2 and Rac3, reducing their affinity for GTP. EHT1864 induces nucleotide release and inhibits nucleotide rebinding. Because all Rac effector interactions are GTP-dependent, EHT1864 is expected to block Rac1 interaction with all effectors (Shutes, 2007). The only known small molecule inhibitor of Cdc42 activation, secramine, inhibits Cdc42 activation only in its prenylated form. Activation of the non-prenylated form of the Cdc42, which does not bind GDI, was unaffected by the inhibitor indicating that secramine inhibits activation of Cdc42 in a Rho GDI-dependent manner. This was supported by the finding that secramine prevents translocation of prenylated Cdc42 to membranes (Pelish, 2006).

Here we describe a bead-based multiplex flow cytometry HTS assay which allowed simultaneous screening of six GTPase targets against ~200,000 compounds in the Molecular Libraries Screening Center Network (MLSCN) library. A potent and selective, reversible non-competitive Cdc42 inhibitor was discovered and SAR of structural analogs explored by synthetic chemistry. The chemical probe and related analogs are biologically active in cell based assays of Cdc42 activation (ELISA) and function (filopodia formation).

2. Project Description

The project goal was to identify selective inhibitory probes for modulating the GTP-binding and activity of representative members of Rho, Ras and Rab GTPase families with > 10-fold inhibitory selectivity and specific emphasis on Cdc42 vs Rac1. As summarized on page 1 and in **Tables 1-2**, the profile of the chemical probe CID2950007 meets the objectives set out below that were agreed to in the approved CPDP:

- A probe should have IC_{50} < 10 μM for Cdc42, Rac1, Rab or Ras and be efficacious at > 50% inhibition in the multiplex in vitro binding assay (Screening Center).

- A probe should have IC_{50} < 5 μM in the primary assay and efficacy of > 65% to advance into secondary assays

- Compounds demonstrating selectivity towards Cdc42 will be assessed in the appropriate microscopy, cell-based assay, as outlined in the flow chart. Compounds having no cytotoxic effects and having a IC_{50} of 10-50 μM will advance into the appropriate assay

- Compounds with Cdc42 activity that meet the above requirements will progress into cell based ELISA assay to determine target activity. Confirmation will result in a probe.

- Probes resulting from this effort will be assessed with respect to their promiscuity on other biological targets using a broad spectrum profiling panel. Also, the chemical stability and solubility of the probe will be evaluated. These data will be the subject of a post-probe enhancement, extended characterization effort.

a) Bioassays

i) Primary HTS and Dose Response Assays

The assays are described in detail in Schwartz et al., 2008 and Surviladze et al., 2010. Individual GST-GTPases (H-Ras wt, Cdc42 wt, Rac1 wt and RacQ61L mutant were purchased from Cytoskeleton and GST-Rab2, GST-Rab7 were purified as described by Schwartz, 2008) were attached to 4 μm diameter glutathione-beads (GSH-beads) distinguished by different intensities of red color (various magnitude of emission at 665 +/- 10 nm with excitation at 635 nm). Bead sets for multiplex assays were custom synthesized by Duke Scientific Corp (Fremont, CA), but may now be ordered from Thermo/Fisher. Individual GTPase-coupled beads were washed twice with 100 μl ice cold NP-HPS buffer [(0.01% (vol/vol) NP-40, 30 mM HEPES pH 7.5, 100 mM KCl, 20 mM NaCl,] supplemented with 1mM EDTA, 0.1% BSA and 1 mM DTT and were pooled together immediately prior to loading of 5 μl of the mixture in each well of the assay plates. Next 0.1 μl of test compounds (1 mM stock in DMSO) were added to individual wells to give a final concentration of 10 μM compound and 1% DMSO, after which 5 μl BODIPY- FL-GTP (200 nM stock in NP-HPSE) was added to each well. Positive controls, contained the bead mixture, 0.1 μl DMSO (1% final) and fluorescent GTP. Negative controls, contained the bead mixture with fluorescent GTP, 0.5 mM unlabeled GTP as a competitor, and 1% DMSO. Plates were incubated on rotator for 40-45 min at 4°C and sample analysis was conducted with a HyperCyt® high throughput flow cytometry platform as described previously (Kuckuck, 2001). Flow cytometric light scatter and fluorescence emission at 530 +/- 20 nm (FL1) and 665 +/- 10 nm (FL8) were collected on a Cyan ADP flow cytometer (Beckman Coulter, Fullerton, CA). Resulting time-dependent data (one file per plate) were analyzed using IDLQuery software to determine the compound activity in each well. Gating based on forward scatter (FS) and side scatter (SS) parameters was used to identify singlet bead populations. Gating based on FL8 emission distinguishes the beads coated with different proteins, and the median fluorescence per bead population was calculated. A compound

was considered a "potential active" if the change in activity was greater then 20% from baseline. Baselines were set to 100% based on measurements from the 1% DMSO containing positive controls as further described in PubChem (PubChem #72). As published (Surviladze et al., 2010), assay performance was robust for all the GTPases selected with for example average Z′ = 0.87 ± 0.04 for Cdc42, 0.85 ± 0.04 for Rac1 wt, and 0.90 ± 0.03 for Rac1Q61L activated mutant. Dose response measurements were also previously described (Surviladze, 2010). Briefly, compounds were serially diluted 1:3 a total of eight times from a starting concentration of 10 mM giving a 9-point dilution series in DMSO. The final concentrations of inhibitors in the assay ranged from 10 nM to 100 μM. Dose–response analyses were examined in the presence of NP-HPS buffer containing: a) 1mM EDTA; or b) 1mM $MgCl_2$. For assays with EDTA we used one multiplex (Rab7 wt, Rab2 wt, H-Ras wt, H-RasG12V, Cdc42 wt, and Cdc42Q61L) and 3 single-plexes (for Rac1 wt, Rac1Q61L and GST-GFP). In experiments including magnesium, six GST-GTPases were assayed simultaneously in a single multiplex (Rac1 wt, Rac1Q61L, RhoA wt, RhoAQ63L, Cdc42 wt and Cdc42Q61L) and 1 nM BODIPY-FL-GTP binding was measured in the presence or absence of the serial drug dilution series. Each dose response series was run in duplicate.

Equilibrium binding assay: wild-type GST-Cdc42 (4 μM) was bound to GSH-beads overnight at 4°C. Cdc42 on GSH-beads was depleted of nucleotide by incubating with 10 mM EDTA containing buffer for 20 min at 30°C, washing twice with NP- HPS buffer, then re-suspended in the same buffer containing 1 mM EDTA/or 1 mM $MgCl_2$, 1 mM DTT and 0.1% BSA. Cdc42 unbound sites were blocked by incubation of protein–bead complex for 15 min at RT. Thirty μl of this suspension incubated with 20 mM inhibitor for 3 min at RT and added 30 μl of various concentrations of ice cold BODIPY-FL-GTP. Samples incubated at 4°C for 45 min and binding of fluorescent nucleotide to enzyme measured using an Accuri flow cytometer. Raw data were exported and plotted using GraphPad Prism software.

ii) Secondary Cell-Based Assays

In vitro Cdc42-GTPγS Complex Formation with PAK-PBD

The Rac/Cdc42 (p21) binding domain (PBD) of the human p21 activated kinase 1 (PAK) specifically binds GTP- and not GDP-bound Cdc42. The PAK-PBD domain can be used to specifically precipitate active, GTP-bound Cdc42. For analysis of the effect of CID2950007/MLS000693334 on the formation of the complex between PAK-PBD and the GTP-bound active form of Cdc42 in vitro, 40 nM His-Cdc42 wt was incubated for 20 min at 30°C with various concentrations of GTPγS in the presence of 1 mM EDTA containing NP-HPS buffer. Reactions were stopped by adding excess $MgCl_2$. The mixture was incubated with 15 μl PAK-PBD beads (Cytoskeleton Inc., Denver, CO) for 1 h then washed 2 times and the PAK-PBD-bead-associated active Cdc42 was analyzed by Western blot probed with a mAb directed against Cdc42 (Cytoskeleton Inc., Denver, CO) and Mouse TrueBlot Ultra: Horseradish Peroxidase anti-mouse IgG (eBioscience. San Diego, CA) followed by ECL detection (Thermo Scientific, Rockford, IL).

G-LISA assays for Cdc42 and RAC1 in 3T3 cells

Swiss 3T3 cells were cultured and serum starved following standard procedures (Cytoskeleton, Inc., Denver, CO). Individual cultures grown in 6-well dishes were incubated with inhibitor for 1 h and subsequently stimulated for 2 min with 10 ng/mL EGF. Cells were washed with ice-cold phosphate buffered saline (PBS) containing calcium and magnesium and further processed for protein and G-LISA assays. Positive controls included Cdc42-GTP or Rac1-GTP provided in the kit and cell lysate prepared from control cells stimulated only with EGF. Negative controls included buffer-only controls and cell lysates prepared from control cells after serum starvation.

Immunofluorescence Staining and Microscopy

Swiss 3T3 cells were grown on coverslips in DMEM plus 10% fetal calf serum (FCS; Gibco) at 37°C in 5% CO_2. Subconfluent cells were starved for 7.5 hrs in DMEM with 0.1% serum then 0% serum for 2 or 3.5 hrs. Cells were treated with inhibitor for 1 h before stimulation. As a positive control, cells were stimulated with 100 ng/ml bradykinin for 10 to 30 min (Kozma, 1995). Cells were washed with phosphate buffered saline, fixed with 4% paraformaldehyde, permeabilized for 5 min with 0.1% Triton X-100 in Tyrode's buffer, blocked for 1 h with 1% BSA in Tyrode's buffer. Cells were stained with Rhodamine Phalloidin for filamentous actin (red) and Hoechst nuclear stain (blue) and then mounted in Prolong Gold. A Zeiss LSM510 META and 63x 1.4NA objective was used to acquire the images. The number of filopodia on each cell was counted.

iii) Center Summary of Results

Table 2. Assessment of CID2950007 in Key Biological Assays (based on CPDP Flow Chart).

Assay Type	Target or System	Effect
Secondary	Nucleotide-depleted Cdc42 wild type, 1 mM MgCl2 and 1.5 nM BODIPY-FL-GTP	IC_{50} = 0.2 μM
Primary	Cdc42 wild type with 1 mM EDTA and 100 nM BODIPY-FL-GTP	IC_{50} = 2.6 μM Range: 0.9-6.8
Primary	Cdc42 activated mutant with 1 mM EDTA and 100 nM BODIPY-FL-GTP	IC_{50} = 5.4 μM Range: 2.1-13.1
Primary	Ras wild type with 1 mM EDTA and 100 nM BODIPY-FL-GTP	IC_{50} = > 100 μM
Primary	Ras activated mutant with 1 mM EDTA and 100 nM BODIPY-FL-GTP	IC_{50} = > 100 μM
Primary	Rab 7 with 1 mM EDTA and 100 nM BODIPY-FL-GTP	IC_{50} = > 100 μM
Primary	Rab 2a with 1 mM EDTA and 100 nM BODIPY-FL-GTP	IC_{50} = > 100 μM
Primary	Rac1 wild type with 1 mM EDTA and 100 nM BODIPY-FL-GTP	IC_{50} = > 100 μM
Primary	Rac1 activated mutant with 1 mM EDTA and 100 nM GTP	IC_{50} = > 100 μM
Secondary	Cdc42 wild type with 1 mM $MgCl_2$ and 100 nM GTP	IC_{50} = 4 μM
Secondary	Cdc42 activated mutant with 1 mM $MgCl_2$ and 100 nM GTP	IC_{50} = 4 μM
Secondary	Rac1 wild type, Rac1 activated mutant, Rho wild type, Rho activated mutant with 1 mM $MgCl_2$ and 100 nM GTP	All IC_{50} > 100 μM
Secondary	Cdc42 wild type, 10 μM 2950007, 1 mM EDTA and 3 to 100 nM BODIPY-FL-GTP	> 50% decrease in B_{max}, minimal effect on K_d for GTP
Secondary	Cdc42 wild type, 10 μM 2950007, 1 mM MgCl2 and 3 to 100 nM BODIPY-FL-GTP	~ 50% decrease in B_{max}, minimal effect on K_d for GTP
Secondary	Nucleotide-depleted Cdc42 wild type, 10 μM 2950007, 1 mM $MgCl_2$ and 3 to 1000 nM BODIPY-FL-GTP	> 50% decrease in B_{max}, minimal effect on K_d for GTP
Secondary	Cdc42 binding to PAK-PBD beads in the presence of 100 to 1000 nM GTPγS	60 to 90% inhibition at 10 μM 2950007
Secondary	Cdc42 GLISA in EGF-stimulated 3T3 cells with 10 μM 2950007	> 50% inhibition
Secondary	Rac1 GLISA in EGF-stimulated 3T3 cells with 10 μM 2950007	< 50% inhibition
Secondary	Bradykinin-stimulated filopodia formation in 3T3 cells with 10 μM 2950007	> 50% inhibition

Primary HTS Assay: Dose Response Data

Binding of 8 different GTPases to 100 nM BODIPY FL-GTP was measured in multiplex format in the presence of 1 mM EDTA in NP-HPS buffer. A GST-GFP control was used to eliminate the possibility of compound effects on GST-protein binding to beads (data not shown). Dose response analysis confirmed that CID2950007 (MLS 00693334) selectively inhibits only Cdc42 binding to BODIPY FL-GTP with IC_{50} ~2 x10 $^{-6}$ M (**Figure 1a**). CID2950007 did not affect BODIPY-FL-GTP binding to Rac1, Rab2, Rab7 or Ras, either wild type or activated mutant proteins, in the concentration range tested i.e. up to 100 µM. Equilibrium binding studies confirmed that BODIPY-FL-GTP affinity for Cdc42 in the presence of 1 mM $MgCl_2$ was significantly enhanced to K_d ~ 0.5-1.5 nM as compared to K_d ~36-40 nM in the presence of mM EDTA (data not shown). Accordingly for inhibition studies with GTPases in the presence of 1 mM Mg^{2+} ions BODIPY-FL-GTP concentration was decreased to 1 nM. **Figure 1b** shows a 6-plex assay with wild-type and constitutively active mutants of Rac1, RhoA, and Cdc42 in the presence of Mg^{2+} ions. CID2950007 was a selective inhibitor for Cdc42 wt and Cdc42 (Q61L) binding to 1 nM BODIPY-FL-GTP in the presence of Mg^{2+} ions with IC_{50} ~4 µM. CID2950007 did not significantly inhibit BODIPY-FL-GTP binding (< 10%) to RhoA or Rac1 up to 100 µM. In summary, using flow cytometry-based multiplex, high throughput screening of BODIPY-FL-GTP binding to Rho family GTPases we identified CID2950007 as a potent Cdc42 inhibitor (IC_{50} = 2 to 4 µM) with an excellent selectivity profile with respect to all other related GTPase family we examined (selectivity ratio= 25 to 50).

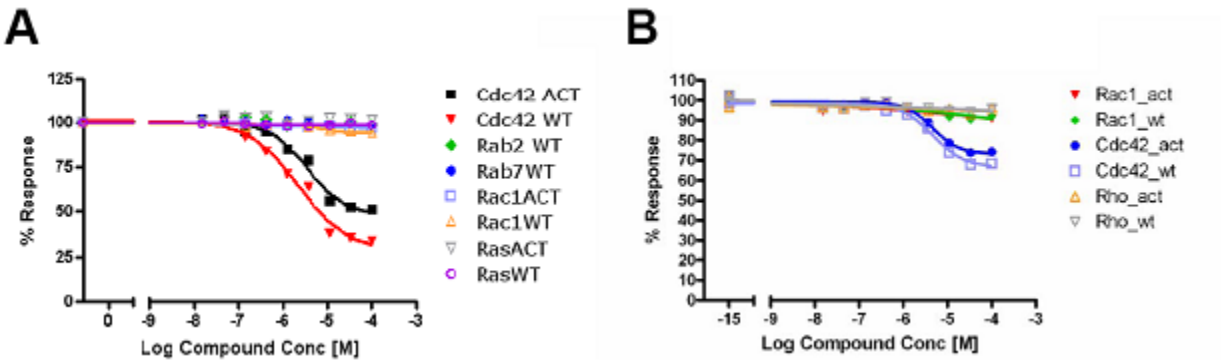

Figure 1. Dose Response for CID2950007 against GTPase family members

The figure shows the inhibition profile of CID2950007/MLS000693334 against 8 GTPases in the presence of 1 mM EDTA and 100 nM BODIPY-FL-GTP (Panel A) and 6 GTPases in the presence of 1 mM Mg^{2+} and 1 nM BODIPY-FL-GTP (Panel B).

Secondary Assays: Mechanism of Action Studies

To confirm the biochemical mechanism of action of CID2950007 for Cdc42 GTPase inhibition, BODIPY-FL-GTP equilibrium binding to wild-type Cdc42 was tested in the presence or absence of CID2950007. Assays were performed with a fixed CID 2950007 concentration of 10 µM and monitoring BODIPY-FL-GTP binding over the range of 3 to 100 nM in the presence of 1 mM EDTA. CID2950007 decreased the B_{max} of GTP-binding, while BODIPY-FL-GTP affinity to wild type Cdc42 at K_d ~4 nM was essentially unchanged by CID2950007 with Kd ~50 nM (Figure 2A). Very similar results were obtained for equilibrium BODIPY-FL-GTP binding to Cdc42 in the presence of 1 mM $MgCl_2$ (Figure 2B). Equilibrium BODIPY-FL-GTP binding was also performed with wild type Cdc42 depleted of endogenous bound nucleotide (GTP or GDP) by standard methods (Zhang, 2005) and in the presence of 1 mM Mg^{2+} with the BODIPY-FL-GTP concentration range extended out to 1 µM to ensure full saturation, as evidenced by both linear and log plots (Figure 2C). These results confirmed definitively the effect of CID 2950007 on B_{max} rather than ligand affinity,

establishing the mode of action as a potent and selective non-competitive Cdc42 inhibitor. The nucleotide-depleted Cdc42 preparation was also tested in the presence of 1.5 nM BODIPY-FL-GTP, 1 mM Mg^{2+} and varying inhibitor concentration (100 nM to 10 μM) to establish an IC_{50} for CID2950007 of 200 nM and for CID2971684 of 400 nM (Figure 2D). A 10-fold lower IC_{50} for CID2950007 on nucleotide-depleted versus partially GTP/GDP bound Cdc42 implies an allosteric/conformational interplay between GTP binding to the active site of Cdc42 and the affinity/occupancy of the newly identified CID2950007 binding site.

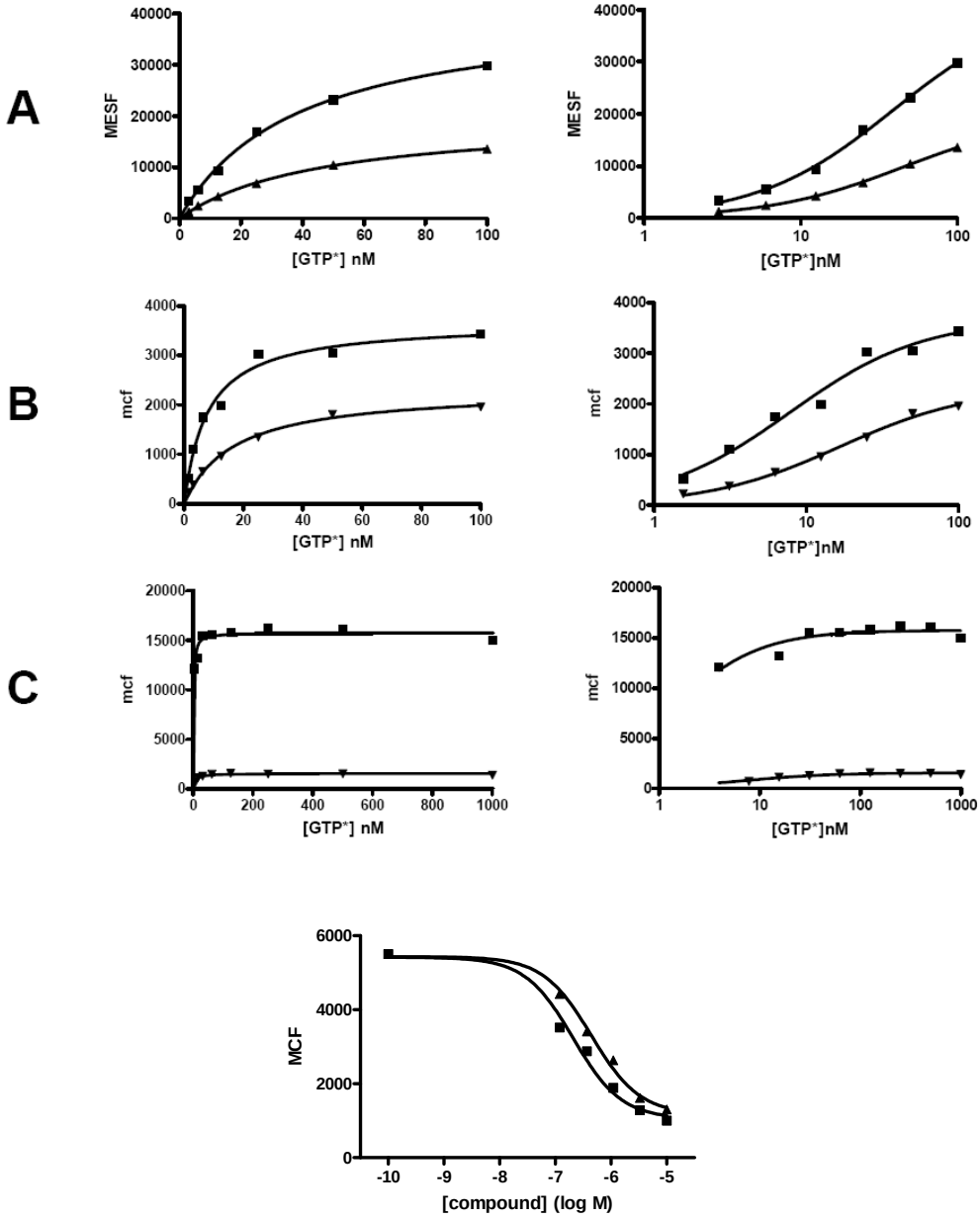

<u>Figure 2.</u> CID2950007 is a Non-Competitive Inhibitor of Cdc42

Equilibrium binding studies were performed with 3-100 nM BODIPY-FL-GTP and wild type Cdc42 plus 10 μM CID 2950007 (triangles) or DMSO vehicle (squares) with either (**A**) 1 mM EDTA or (**B**) 1 mM Mg^{2+} ions. In (**C**) BODIPY-FL-GTP was tested from 10 nM to 1 μM in the presence of Mg^{2+} ions using 10 μM CID2950007 and nucleotide-depleted Cdc42. The principal mode of action is a decrease in GTP binding sites (B_{max}) rather than a change in GTP affinity. In (**D**), IC_{50} for CID 2950007 (squares) of 200 nM was determined using nucleotide-depleted Cdc42, 1 mM Mg^{2+} ions and 1.5 nM BODIPY-FL-GTP. A related analog CID 2971684 had IC_{50} = 400 nM (triangles) in this assay.

Secondary Biochemical Assay – GTPγS bound Cdc42:PAK-PBD Complex Formation

Since CID2950007 inhibits total GTP binding to Cdc42 we tested whether it could prevent association of GTPγS-bound Cdc42 with PAK-PBD-GST beads using a pull down strategy and Western blot for Cdc42. As shown in lanes 1 to 3 of **Figure 3**, in the presence of DMSO robust association and pull down of active Cdc42 was achieved in the presence of 100, 500 and 1000 nM GTPγS. As shown in lanes 4 to 6, incubation with 10 μM CID2950007 almost completely blocked the association of Cdc42 with PAK-PBD promoted by 100 and 500 nM GTPγS (> 90% by densitometry) and was partially effective (>50% inhibition) in the presence of 1000 nM GTPγS. These results are consistent with the equilibrium binding studies showing that CID2950007 inhibits GTP binding to Cdc42.

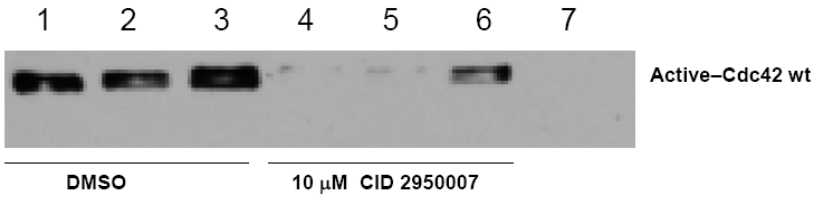

Figure 3. CID2950007 Inhibits Cdc42 association with PAK-PBD. 40 nM His-Cdc42 wt was incubated for 20 min at 30°C with various concentrations of GTPγS in the presence of 1 mM EDTA and DMSO alone (lanes 1-3) or 10 μM CID2950007 (lanes 4-6). Reactions were stopped by adding excess Mg^{2+}. The mixture was incubated with 15 μl PAK-PBD beads (Cytoskeleton, Inc.) for 1 h, washed 2 times and active Cdc42 was analyzed by Western blot probing with a mAb directed against Cdc42. Lanes 1 and 4: 100 nM GTPγS; lanes 2 and 5: 500 nM GTPγS; lanes 3 and 6: 1000 nM GTPγS. Lane 7 is a specificity control incubation containing PAK-PBD beads but no added Cdc42.

Secondary Cell-Based Assays

Having established the potency, selectivity and mechanism of action of CID2950007 as a Cdc42 inhibitor, the activity profile of this innovative probe was tested using appropriate secondary cell-based assays in the flow chart.

GLISA assays for CTP-Cdc42 and GTP-Rac Content in EGF-stimulated 3T3 cells

Figure 4 shows the results for Cdc42 (**left panel**) and Rac1 (**right panel**) G-LISA assays obtained with Swiss 3T3 fibroblasts pre-incubated for 1 hour with 1 or 10 μM CID 2950007/MLS0000693334 and then stimulated for 2 min with 10 ng/ml epidermal growth factor (EGF). Comparative data for 5 additional synthetic analogs of CID2950007 that were developed during SAR analysis for probe optimization are also shown. Data are normalized to the amount of GTP-bound Cdc42 or Rac-1 in the presence of EGF. There was a modest, but reproducibly measurable increase (~40-50%) in GTP-Cdc42 content of 3T3 cells following EGF stimulation consistent with published reports. The EGF-stimulated increase in GTP-Cdc42 was inhibited in the presence of 10 but not 1 μM CID2950007. This suggests robust intracellular inhibition of Cdc42 GTP-binding and activation by the probe. The close analogs CID13927310/SID85148307 and CID44143700/SID85148308 had a similar profile to CID2950007 in the G-LISA, whereas analogs CID44143703/SID85148312, CID44143698/SID85148304 and CID13927312/SID85189505 either had no reproducible effect or appeared to cause a counterintuitive increase in GTP-Cdc42 content. Assay for GTP-Rac1 content by G-LISA showed a more robust signal to noise ratio of ~ 5:1 for EGF stimulation versus baseline conditions (no EGF). Surprisingly, despite no evidence of any Rac-1 GTPase inhibition up to 100 μM in the biochemical primary assays, there was a partial

~ 30-50% inhibition of the EGF-stimulated increase in intracellular GTP-Rac-1 content in cells pre-incubated with 1-10 μM CID2950007 and several related analogs. Although hard to interpret, the results may imply off-target effects not related to direct Rac1 inhibition but via intracellular targets regulating Rac1 activation status. Such a hypothesis could be examined by broader MDS pharma testing against diverse receptor and kinase targets. The analog CID44143700/SID85148308 had minimal effects in the Rac-1 assay at 1 or 10 μM.

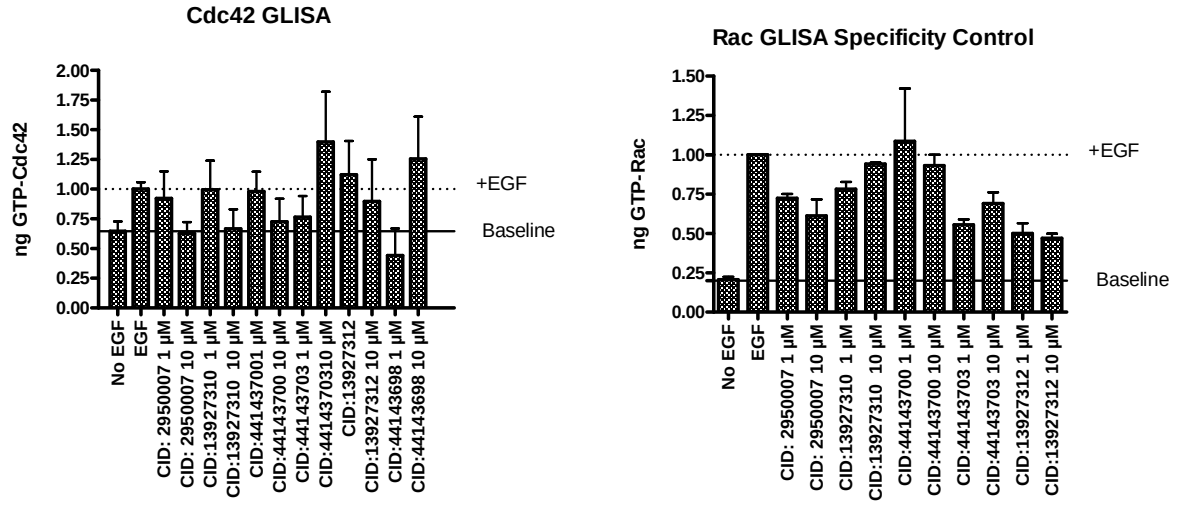

Figure 4. CID2950007 activity in cell-based GTP-Cdc42 and GTP-Rac1 content G-LISA assays in 3T3 cells stimulated with EGF. 3T3 cells were serum starved in 6-well dishes and incubated with inhibitors for 1 h then stimulated for 2 min with 10 ng/mL EGF. Cells were washed with ice-cold phosphate buffered saline containing Ca^{2+} and Mg^{2} and processed for G-LISA assay. Positive controls included GTP-Cdc42 or GTP-Rac1 provided in the kit and lysates prepared from control cells stimulated only with EGF. Negative controls included buffer-only controls and lysates prepared from control cells after serum starvation.

Bradykinin-induced filopodia formation

To further examine the probe in a cell based assay of activated Cdc42 function we examined bradykinin-induced filopodia (peripheral actin microspikes, PAM) formation in 3T3 cells. This cellular response was shown to be Cdc42-dependent in 3T3 cells (Kozma et al., 1995) and recently to be ablated by Cdc42 gene silencing in mouse embryonic fibroblasts (Yang et al., 2006). The results are shown in **Figure 5**. **Panel A** shows confocal images of a resting 3T3 cell with few filopodia, robust filopodia formation in a bradykinin-stimulated cell and attenuation of this response by prior incubation with 10μMCID2950007. **Table 3** and **Figure 5 Panel B** shows the mean number of PAM/3T3 cell for cells treated with 0.1 % DMSO vehicle alone (resting), resting + 10 μM CID2950007 without bradykinin, bradykinin stimulation for either 10 or 15 min and bradykinin stimulation with pre-incubation of cells for 60 min with CID2950007. Data shown are for a minimum of 10 and up to 17 cells analyzed per condition. A robust increase of mean PAM/cell induced by bradykinin versus vehicle control at both 10 and 15 min (3-4-fold) was strongly attenuated in cells pre-treated with CID2950007

Table 3. CID 2950007 Inhibits Filopodia Formation in 3T3 Fibroblasts

	# Filopodia / cell (mean +/- s.e.m.)	# cells evaluated
Resting 3T3 cells	5.1 +/- 3.1	10
Resting + 10 μM CID2950007	2.9 +/- 3.7	11
200 ng/ml bradykinin, 10 min	17.8 +/- 4.0	17
200 ng/ml bradykinin, 10 min	22.9 +/- 6.1	10
10 μM CID2950007 + bradykinin, 10 min	8.6 +/- 3.2	10
10 μM CID2950007 + bradykinin, 15 min	2.5 +/- 1.5	13

A

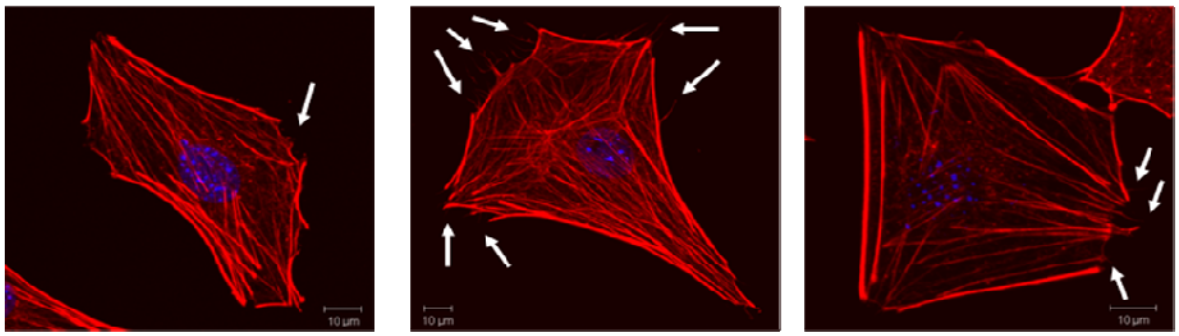

B

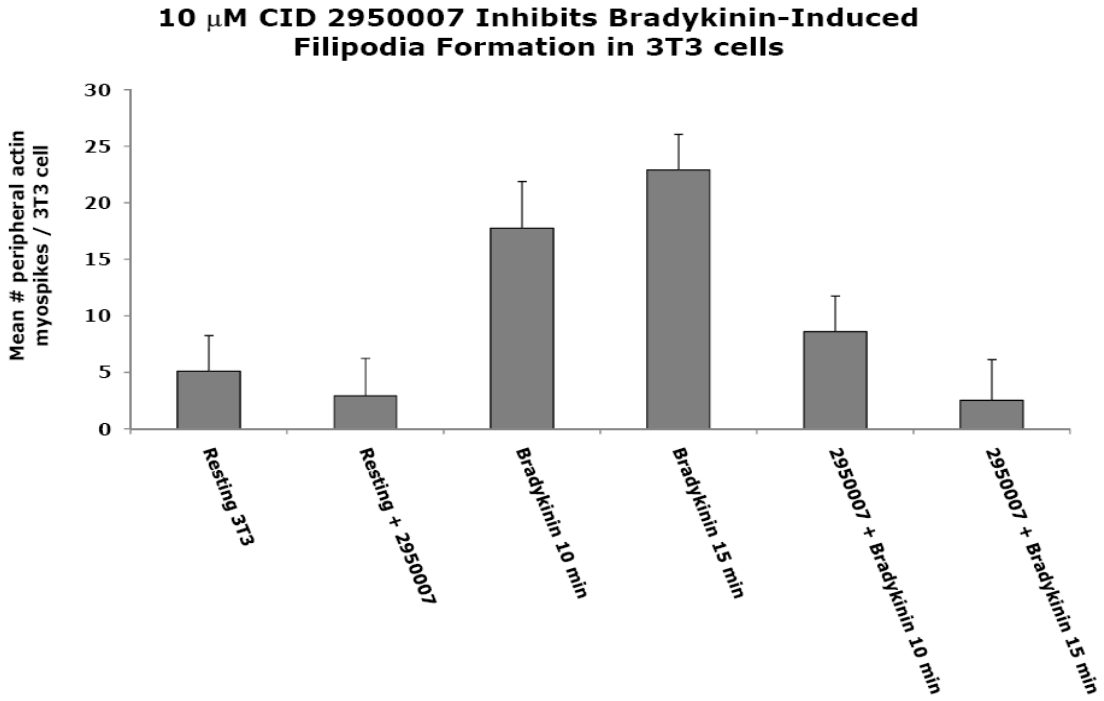

Figure 5. CID 2950007 inhibits bradykinin-induced filopodia formation.
Panel A shows confocal images with a few peripheral actin myospikes (PAM i.e. filopodia – marked by arrows) on a resting Swiss 3T3 cell, a robust increase in PAM on a cell treated with 200 ng/ml bradykinin and decreased PAM in a cell pre-treated with 10 μM CID2950007. Panel B shows the mean number of PAM counted on a minimum of at least 10 individual 3T3 cells either resting (with 0.1% DMSO), resting for 60 min with 10 μM CID2950007, treated for 10 or 15 min with 200 ng/ml bradykinin or 60 min with CID2950007 followed by bradykinin. Data are the mean +/- s.e.m. for a minimum of 10 and up to 17 individual cells analyzed.

PubChem Assays and General Selectivity Profile

A general pharmacological screen for the specificity/selectivity of CID 2950007 / MLS 0000693334 at physiologically relevant targets will be performed at MDS Pharma for publication purposes. A 'Bioactivity Analysis' search in PubChem revealed that CID 2950007 / MLS 0000693334 has been tested in 263 assays and is active in just 8 of these, of which 4 are bead-based GTPase assays described in this probe report (AID 761, 1333, 1334 and 1337). The remaining 4 assay "hits" are shown below:

Yeast-based HTS Assays

a) AID 868: "A screen for inhibitors of the budding yeast RAM network."

The compound is described as a confirmed active but no IC_{50} is given. The RAM pathway in budding yeast controls polarized growth, cell proliferation and gene expression. Of interest both the RAM1 and RAM2 gene products in yeast regulate prenylation of GTPase pathways (He, 1991).

b) AID 1362: "Screening for compounds that inhibit mitochondrial fusion using a yeast model system as a primary screening tool".

The compound is described as a confirmed active but no IC_{50} is given. Interestingly it is stated in the assay description that "we have identified proteins that are required for mitochondrial fission and fusion...the key proteins among these are three dynamin-related proteins (DRPs), which are large self-assembling GTPases".

Given the conserved cellular functions of small GTPases across phyla and the 80% sequence identity between human and *S. cerevisiae* Cdc42 a hit in the above GTPase-dependent primary assay systems would not be unexpected.

Mammalian Cell Based Assays

AID 1885 and AID 2044: "HTS to Identify Inhibitors of *T. Cruzi* Replication."

This is a 90-hour assay for parasite replication in 3T3 cells, *nota bene* the same cell line we have used for filipodia experiments. CID 2950007 / MLS 0000693334 is described as active in the primary *T. cruzi* replication HTS and to have IC_{50} = 2.8 μM in a confirmed dose response. This cellular potency is in the range we have noted for the G-LISA and filipodia assays in 3T3 cells (IC_{50} <10 μM). Rho GTPases, including Cdc42, are implicated in *T. cruzi* invasion in MDCK cells (Dutra 2005) and Cdc42 is involved in the invasion / replication / infection processes for viruses (Van den Broek, 2010) and other pathogens, such as pneumococci (Agarwal V. 2009).

In conclusion, CID 2950007 / MLS 0000693334 is highly selective Cdc42 chemical probe within the rho GTPase family we have tested and appears to have broad pharmacological specificity based on assay data compiled in the MLPCN databases.

Probe Optimization

The primary HTS screen identified CID 2950007/MLS000693334 as a promising hit compound (**Figure 6**). The compound showed inhibitory potency and selectivity for Cdc42 WT and Cdc42 ACT and was devoid of any significant activity for the other GTPases surveyed.

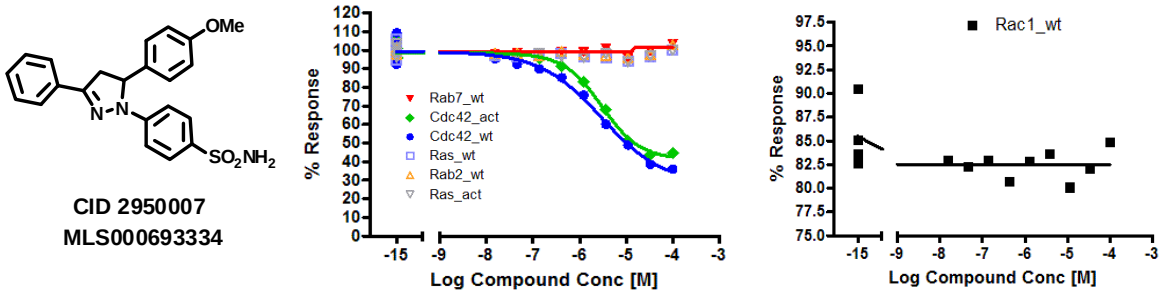

Figure 6. Hit scaffold and dose response curves illustrating selectivity for Cdc42

Over the course of the SAR expansion and testing, this substance was assayed on six occasions. The substance was first sourced from BioFocus DPI as part of the cherry pick selection in the HTS phase. The compound was then ordered from commercial sources (ChemBridge) as part of a solid retest, and finally, the compound was prepared at the KU SCC and submitted for repeated assay comparison as new analogs were generated for the primary assay. An average of the tabulated potency and efficacy was used as the benchmark against which analogs were compared. The data for the compiled survey of this substance is presented in **Table 4**.

Table 4. Summary of data from primary assay collected on hit compound CID 2950007/MLS000693334

Source	Identifier	Cdc42 ACT EC_{50} µM	Cdc42 ACT Efficacy	Cdc42 WT EC_{50} µM	Cdc42 WT Efficacy
DPI	MLS000693334	8.0	70%	3.2	82%
Chembridge	SID57644019	2.1	54%	1.2	78%
Chembridge	SID 57644019	2.1	59%	1.2	81%
KU SCC	SID 57578341	3.4	57%	0.85	51%
KU SCC	SID 57644019	3.5	53%	2.2	71%
KU SCC	SID 57578387	13.1	46%	6.7	50%
Average Value		**5.4**	**57%**	**2.6**	**69%**

Averaged data collected in the primary dose response assay for the hit scaffold satisfied the criteria set for passing into secondary assays. As such, this compound was further evaluated while SAR was initiated on the series.

Compounds of the same chemotype in the HTS screen lacked significant inhibitory activity and/or efficacy for Cdc42. An SAR strategy was devised that independently targeted the

four rings of the structure. This effort was done with the aim of preserving the selectivity and improving potency for Cdc42 as determined by the primary dose response assay, enhancing efficacy of 65% or better in the primary assay for Cdc42 WT, and demonstrating suitable activity in secondary assays.

The parent structure was dissected into four regions for medicinal chemistry and SAR follow-up (**Figure 7**). Modifications and their impact are discussed in detail below.

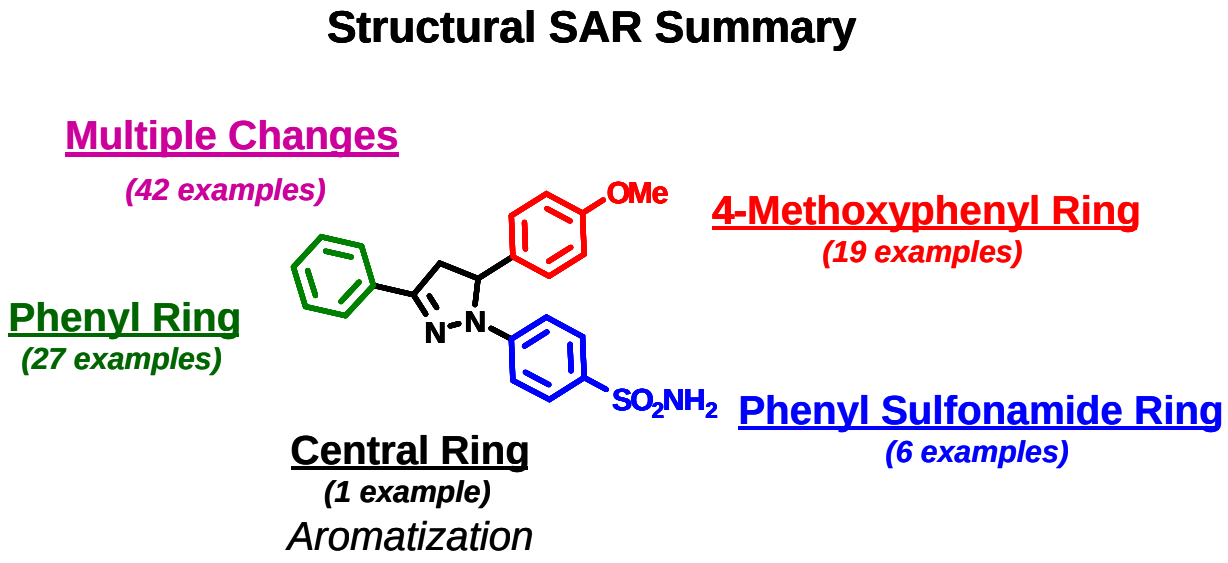

Figure 7. Overview of structural variations resulting from SAR efforts

Modification of the *N*-phenyl-4-sulfonamide moiety: Bioisosteric replacement of the sulfonamide functional group produced compounds devoid of any significant inhibitory GTPase activity. Exchange of the phenylsulfonamide for a phenyl ring substituted in the 4-position with a sulphone (4-SO_2CHF_2), carboxylic acid (4-CO_2H), amide (4-CO_2NH_2), or nitro (4-NO_2) group resulted in complete loss of inhibitory activity. Removal of the sulfonamide or substitution with alkyl or alkoxy groups or halides, in combination with other changes on the structure, also dramatically attenuated the potency or efficacy (i.e., flat dose response curves) as compared to the hit compound. Migration of the sulfonamide group to alternate 2- or 3- positions on the phenyl ring produced analogs with inferior potency and efficacy profiles. As such, this key functionality was quickly assessed as a critical component of the scaffold that would be held constant as other structural features were surveyed. Representative PubChem CIDs for these changes are 2865225, 5181298, 2952426, 44216863, and 44246341.

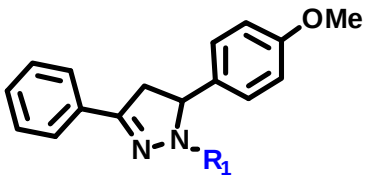

Modification of the phenyl moiety: Systematic, single point changes on this appendage of the parent scaffold resulted in 27 analogs. Substitutions made in concert with other structural alterations afforded an additional 27 analogs. Modifications focused on a survey of the electronic and spatial requirements for this region of the scaffold. The addition of substituents in any of the available positions on the phenyl ring generally produced analogs with decreased efficacy compared to the parent, thus generating very shallow and broad dose response curves. A few exceptions were found. Installation of a 2-methoxy group on the phenyl ring produced

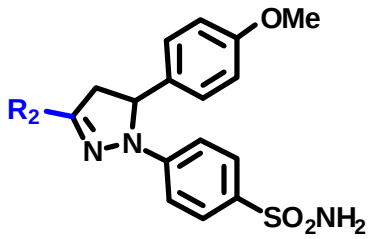

a compound with CID 44143702 which showed similar potency to the hit compound with Cdc42 ACT/WT activity of 5.5 μM (42% efficacy) and 6.0 μM (59% efficacy), respectively. Replacement of the phenyl group with a 2-thiophene group gave compound CID44143712 with results similar, but not superior to, those observed with the parent hit (**Table 5**). The use of a 3-thiophene group resulted in a loss of potency and efficacy compared to the hit compound. Incorporation of alkyl groups in place of an aryl moiety was not beneficial.

Table 5. Selected examples of SAR from modifying the phenyl moiety (R_2) of the MLS000693334 scaffold

Entry	R_2	PubChem CID	Cdc42 ACT EC_{50} μM	Cdc42 ACT Efficacy	Cdc42 WT EC_{50} μM	Cdc42 WT Efficacy
1	2-OMe-phenyl	44143702	5.5	42%	6	59%
2	3-OMe-phenyl	44143698	1.6	30%	1.5	50%
3	4-OMe-phenyl	15201811	2.5	23%	2.6	38%
4	2-thiophene	44143712	4	42%	2.9	57%
5	3-thiophene	44143713	7.3	33%	7.3	47%
6	methyl	14870296	> 100	16%	> 100	17%
7	tert-butyl	44193701	> 100	29%	> 100	33%

Modification of the 4-methoxyphenyl moiety: Systematic, single-point substitution of this particular phenyl ring (**R_3**) afforded 19 compounds with various electronically activating or deactivating groups. Changes made on this ring in combination with other structural modifications afforded an additional 39 analogs. Variations in this region yielded several compounds with a comparable or improved profile as compared to the parent hit in the primary dose response assay. Results of this effort are summarized in **Table 6**.

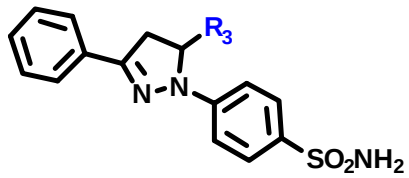

Table 6. Selected examples of SAR from modifying the 4-methoxyphenyl moiety (R_3) of the MLS000693334 scaffold

Entry	R_3	PubChem CID	Cdc42 ACT EC_{50} μM	Cdc42 ACT Efficacy	Cdc42 WT EC_{50} μM	Cdc42 WT Efficacy
1	phenyl	2837695	16.8	44%	31.6	56%
2	2-Br-phenyl	44216862	> 100	NA	> 100	NA
3	3-Br-phenyl	44143703	3.7	50%	3.3	55%
4	4-Br-phenyl	13927312	1.7	52%	1.1	56%
5	2-Cl-phenyl	44193697	7.4	27%	7.2	39%
6	3-Cl-phenyl	44193696	3.6	51%	3.3	64%
7	4-Cl-phenyl	13927311	3.6	56%	2.8	69%
8	3-F-phenyl	12005853	9.6	58%	4.9	71%
9	2-MeO-phenyl	42628035	78.9	34%	22.5	45%
10	3-MeO-phenyl	44143701	4.3	39%	4.8	53%
11	2-Me-phenyl	44143704	13.6	42%	16.6	55%
12	3-Me-phenyl	44143700	5.3	50%	5.0	55%
13	4-Me-phenyl	13927310	5.0	46%	5.0	66%
14	3,4-diMeO-phenyl	2971684	6.1	56%	5.7	75%

Substitutions at the 2-position of this phenyl ring resulted in deteriorated potency as compared to those same substitutions at the 3- or 4-position of the same ring (entries 2, 5, 9, and 11 in **Table 6**). Shaded entries represent analogs with sufficiently interesting potency and efficacy profiles that they were considered for secondary assay assessment.

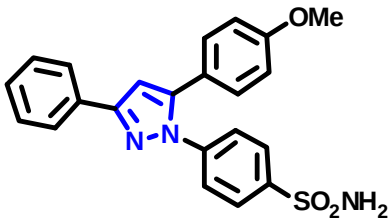

CID 14199398

Modification of the central dihydropyrazoline core: This scaffold exists in a puckered conformation as a result of the dihydropyrazoline ring. Compounds possessing an aromatic pyrazoline ring with similar aromatic appendages have been the subject of clinical significance (Penning, 1997). In order to assess the effect of flattening out the scaffold in the context of GTPase activity, the analog featuring an oxidized central ring was prepared. The efficacy was sub-optimal, resulting in almost a flat dose response curve.

Tandem structural modifications (changes in more than one region at a time): Many of the compounds in this category were screened as a part of a commercially available set and did not possess structural elements that we later discovered to be critical to effective inhibition of Cdc42. In most cases, these compounds lead to flat dose response curves or activation instead of the desired inhibitory activity. However, a few compounds were deliberately prepared as a means to incorporate structural features that were beneficial in previous SAR rounds as described above. One example was CID 44216842, featuring a combination of the best of what was learned from single point changes made during the course of SAR exploration (Figure 8). Knowing that a boost in potency was observed with these substituents, the 4-bromophenyl (R_3) and 3-methoxyphenyl (R_2) aryl groups were incorporated into the same analog. The result was a sub-micromolar potent, Cdc42 ACT/WT selective GTPase inhibitor, devoid of Rac activity. The efficacy of this analog was almost equivalent to that of the parent observed for Cdc42 ACT and *ca*. 10% less than that of the parent for Cdc42 WT.

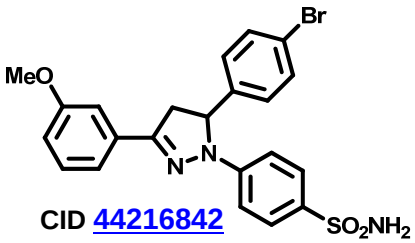

CID 44216842

PubChem CID	Cdc42 ACT EC_{50} µM	Cdc42 ACT Efficacy	Cdc42 WT EC_{50} µM	Cdc42 WT Efficacy
44216842	0.66	55%	0.40	57%

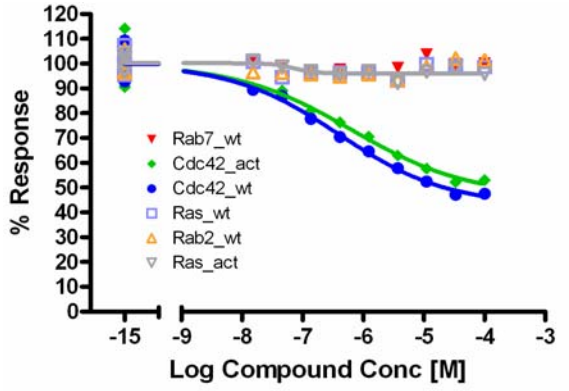

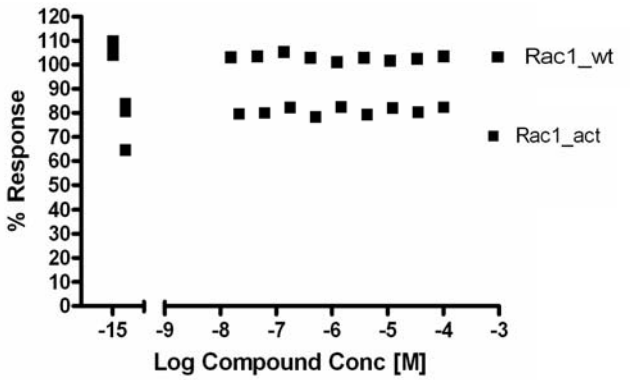

Figure 8. Primary dose response assay data for CID 44216842

The throughput of the secondary GLISA assay was low (AID 2375). As such, a handful of compounds were analyzed. Compounds selected for evaluation included those structures shown in Figure 9.

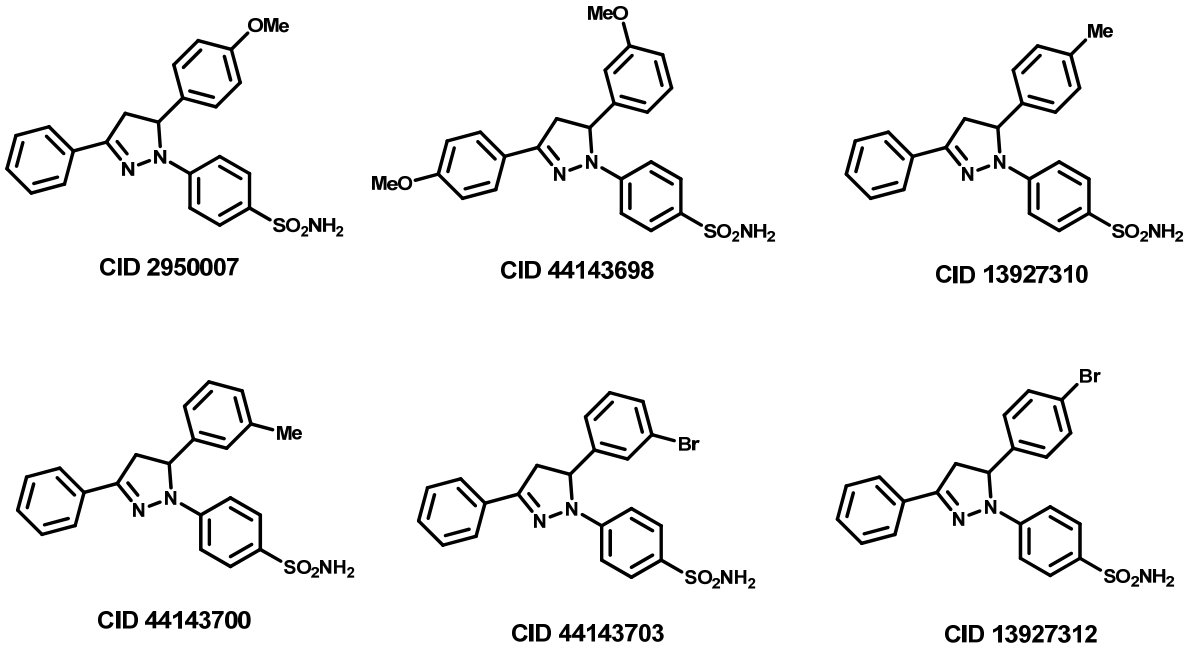

Figure 9. Selected compounds for GLISA analysis (AID 2375)

The results of the GLISA assay determined that the parent compound (MLS000693334, CID 2950007), and compounds with CIDs 44143700 and 13927310 showed a significant response at 10 μM to inhibit Cdc42 with similar potency and efficacy to each other

3. Probe Information and Characteristics

a. CHEMICAL IUPAC NAME:

4-[3-(4-methoxyphenyl)-5-phenyl-3,4-dihydropyrazol-2-yl]benzenesulfonamide **[ML141]**

b. STRUCTURE AND STEREOCHEMISTRY: (Racemic)

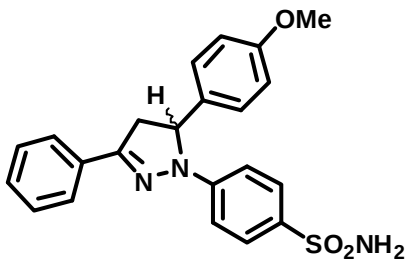

c. STRUCTURAL VERIFICATION INFORMATION OF PROBE MLS000693334 (CID: 2950007):

See Section h. Synthetic Route and Characterization below.

d. PUBCHEM SID AND CID OF PROBE:

Probe PubChem CID: 2950007
Probe PubChem Original SID (Chembridge): 57644019
Probe PubChem NEW SID: 57578341
Probe NEW MLS Number: **MLS002699035**

e. SUPPLIERS, VENDORS AND CONTACT INFORMATION:

VENDOR	ChemBridge Screening Library
LIST DATE	January 2010 (SciFinder)
ORDER NUMBER	7725949
CHEMICAL NAME AS USED BY VENDOR	4-[5-(4-methoxyphenyl)-3-phenyl-4,5-dihydro-1H-pyrazol-1-yl]benzenesulfonamide
REGISTRY NUMBER	71203-35-5
PRICING	1 mg / $40
COMPANY INFO	ChemBridge Corporation 16981 Via Tazon, Suite G San Diego, CA, 92127 USA Phone: (800) 964-6143 Phone: (858) 451-7400 Fax: (858) 451-7401 Web: http://www.chembridge.com

This compound is also available from the University of Kansas, Specialized Chemistry Center. If you are interested in the probe compound, itemized analogs or other derivatives of this scaffold, please contact our Compound Curator and reference the PubChem SID, if available:

Mr. Patrick Porubsky
KU SCC Compound Curator
Structural Biology Center
Lawrence, KS 66047
pporubsky@ku.edu
(785) 864-6167

f. MLS NUMBER UPON SUBMISSION TO THE MLSMR:

Date: February 22, 2010

New MLS Assignments of Probe
MLS002699035 CID: 2950007 Original SID: 57578341

New MLS Assignments of Related Analogs:

MLS002699036 CID: 44143698 Original SID: 85148304

MLS002699037 CID: 44143703 Original SID: 85148312

MLS002699038 CID: 13927312 Original SID: 85189505

MLS002699039 CID: 44143700 Original SID: 85148308

MLS002699040 CID: 13927310 Original SID: 85148307

g. MODE OF ACTION

The probe is a potent, selective and reversible non-competitive inhibitor of Cdc42 GTPase as determined by a bead-based Cdc42/GTP substrate assay. The inhibitor potency is ~ 2 μM in the presence of EDTA and 100 nM BODIPY-FL-GTP and ~ 200 nM in the presence of 1 mM Mg^{2+} ions and 1 nM BODIPY-FL-GTP. No appreciable inhibitory activity up to 100 μM was observed with Rac1, Rab2, Rab7 or Ras. This Cdc42-specific probe has low micromolar activity (1-10) in qualitative and semi-quantitative cell-based assays of such as GLISA assay for active GTP-bound Cdc412/PAK-PBD complex and Cdc42-dependent function in filopodia formation in 3T3 cells. The probe has not been extensively characterized for general pharmacological selectivity against physiologically relevant targets and its in vivo profile is not known.

h. SYNTHETIC ROUTE:

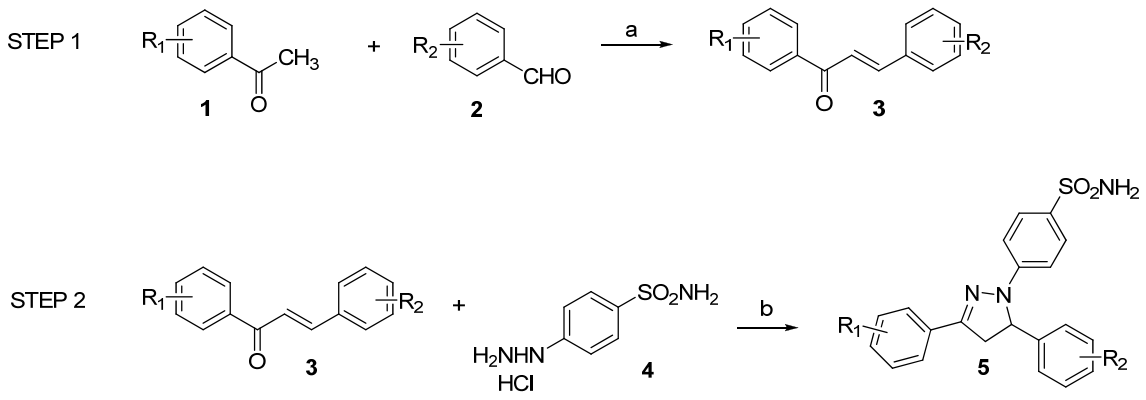

Reagents: (a) NaOH, EtOH, H_2O, 0°C to rt, 12h-36h; (b) microwave, with or without AcOH, 120 - 160°C, 1-2 h.

Figure 10. General synthetic scheme for the synthesis of dihydropyrazolines

General experimental and analytical details: ^{1}H and ^{13}C NMR spectra were recorded on a Bruker AM 400 spectrometer (operating at 400 and 101 MHz respectively) in $CDCl_3$ with 0.03% TMS as an internal standard or DMSO-d_6. The chemical shifts (δ) reported are given in parts per million (ppm) and the coupling constants (J) are in Hertz (Hz). The spin multiplicities are reported as s = singlet, br. s = broad singlet, d = doublet, t = triplet, q = quartet, dd = doublet of doublet and m = multiplet. The LCMS analysis was performed on an Agilent 1200 RRL chromatograph with photodiode array UV detection and an Agilent 6224 TOF mass spectrometer. The chromatographic method utilized the following parameters: a Waters Acquity BEH C-18 2.1 x 50mm, 1.7μMcolumn; UV detection wavelength = 214nm; flow rate = 0.4ml/min; gradient = 5 - 100% acetonitrile over 3 minutes with a hold of 0.8 minutes at 100% acetonitrile; the aqueous mobile phase contained 0.15% ammonium hydroxide (v/v). The mass spectrometer utilized the following parameters: an Agilent multimode source which simultaneously aquires

ESI+/APCI+; a reference mass solution consisting of purine and hexakis(1H, 1H, 3H-tetrafluoropropoxy)phosphazine; and a make-up solvent of 90:10:0.1 MeOH:Water:Formic Acid which was introduced to the LC flow prior to the source to assist ionization. The melting point was determined on an Electrothermal Mel-Temp melting point apparatus.

Chalcone synthesis (STEP 1): For analogs of **CID: 2950007/** MLS000693334, chalcones were synthesized as shown in step 1 of Figure 10. The general procedure is described as follows: To a stirred solution of NaOH (1.2 eq, 6.25 mmol, 0.25 g) in H_2O (2.5 mL) was added the ketone (1eq, 5.0 mmol) in EtOH (1.5 mL). The solution was cooled to 0°C and then the aldehyde (1eq, 5.0 mmol) was gradually added. Once the addition was complete, the mixture was allowed to warm to room temperature and was stirred for 12 – 36 hours, until judged complete by LCMS. The reaction was quenched by the addition of NH_4Cl sat. solution (4 mL) and extracted with EtOAc (2 x 8 mL). The organic layer was separated, combined, and dried over Na_2SO_4. Filtration and concentration of the solvent *in vacuo* afforded the desired product in sufficient purity for further use (Isleyen, 2007).

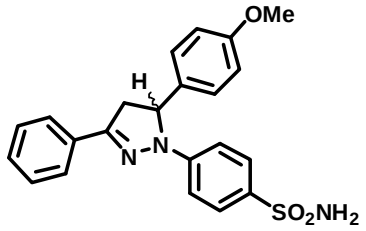

Probe: MLS000693334; CID: 2950007

4-[3-(4-methoxyphenyl)-5-phenyl-3,4-dihydropyrazol-2-yl]benzenesulfonamide:
For the synthesis of this compound, the requisite chalcone starting material was commercially available. 4-Methoxychalcone (**3**, R_1 = H, R_2 = 4-OMe, CAS# 959-33-1) was purchased from Sigma-Aldrich and 4-hydrazinobenzene-1-sulfonamide hydrochloride (**4**, CAS# 17852-52-7) was purchased from Acros Organics. **(STEP 2)**: To a 20 mL microwave vial was added 4-methoxychalcone (0.238 g, 1.00 mmol, 1 eq), EtOH (200 proof, 10 mL), 4-hydrazinobenzene-1-sulfonamide hydrochloride (0.252 g, 1.13 mmol, 1.1 eq), and glacial AcOH (0.29 mL, 5.0 mmol, 5 eq). The vessel was sealed and then submitted to microwave irradiation at 150 °C for 1 h. Once the reaction mixture had cooled to room temperature, the cap was removed and the vessel was placed in a dry-ice/acetone bath. While stirring, hexane (10 mL) was added, and the resulting precipitate was collected by filtration. The precipitate was rinsed with hexane (3 × 10 mL) and then the solid was transferred to another flask and recrystallized from EtOH (6 mL). The solid was filtered, rinsed with hexanes (3 × 10 mL) and dried to afford 4-(5-(4-methoxyphenyl)-3-phenyl-4,5-dihydro-1*H*-pyrazol-1-yl)benzenesulfonamide (0.150 g, 37% yield, 97% purity by LCMS at 254 nm) as white needles. ^{1}H NMR (400 MHz, DMSO-d6) δ 7.80 (m, 2H), 7.58 (d, *J* = 9.0 Hz, 2H), 7.43 (m, 3H), 7.18 (d, *J* = 8.7 Hz, 2H), 7.09 (d, *J* = 9.0 Hz, 2H), 7.02 (s, 2H), 6.90 (d, *J* = 8.7 Hz, 2H), 5.60 (dd, *J* = 12.0, 5.1 Hz, 1H), 3.95 (dd, *J* = 17.6, 12.0 Hz, 1H), 3.71 (s, 3H), 3.17 (dd, *J* = 17.7, 5.1 Hz, 1H). ^{13}C NMR (101 MHz, DMSO-d6) δ 158.59, 149.58, 145.87, 133.48, 132.98, 131.83, 129.24, 128.69 (x 2), 127.06 (x 2), 126.99 (x 2), 126.02 (x 2), 114.42 (x 2), 112.02 (x 2), 61.88, 55.02, 42.97. Compounds of this chemotype submitted to LCMS analysis routinely showed a parent mass and/or a parent mass - 2, the latter of which resulted presumably due to an analytical instrument artifact that resulted in oxidation/aromatization of the central dihydropyrazoline ring on the LCMS column, in the MS detector, or both. In this case, both ions were observed in the same peak. LCMS

retention time: 3.057 min. HRMS *m/z* calculated for $C_{22}H_{21}N_3NaO_3S$ [M^++Na]: 430.1196, found 430.1180. For aromatized/oxidized signal, HRMS *m/z* calculated for $C_{22}H_{20}N_3O_3S$ [M^+-2+1] 406.1225, found 406.1217. White needles, mp 185-187 °C. (Faid-Allah, 1988).

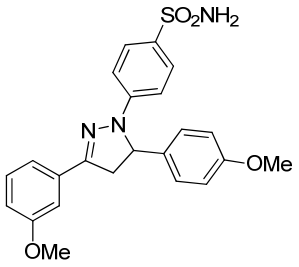

Analog: MLS002699036; CID: 44143698

4-[5-(3-methoxyphenyl)-3-(4-methoxyphenyl)-3,4-dihydropyrazol-2-yl]benzenesulfonamide: This analog was prepared as depicted in steps 1 and 2 in Figure 10. Isolated 176mg, 0.40 mmol, 96% yield, as a yellow solid. ^{1}H NMR (400 MHz, DMSO-d6) δ 7.58 (d, *J* = 9.0 Hz, 2H), 7.36 (m, 2H), 7.32 (d, *J* = 1.8 Hz, 1H), 7.17 (d, *J* = 8.8 Hz, 2H), 7.09 (d, *J* = 9.0 Hz, 2H), 7.02 (s, 2H), 6.98 (m, 1H), 6.90 (d, *J* = 8.8 Hz, 2H), 5.59 (dd, *J* = 12.0, 5.1 Hz, 1H), 3.92 (dd, *J* = 17.7, 12.1 Hz, 1H), 3.82 (s, 3H), 3.70 (s, 3H), 3.17 (dd, *J* = 17.7, 5.1 Hz, 1H). ^{13}C NMR (101 MHz, DMSO-d6) δ 159.45, 158.61, 149.52, 145.83, 133.49, 133.21, 133.03, 129.83, 127.07 (x 2), 127.01 (x 2), 118.59, 115.23, 114.44 (x 2), 112.08 (x 2), 110.96, 61.90, 55.21, 55.05, 43.04. LCMS retention time: 3.050 min. HRMS *m/z* calculated for $C_{23}H_{23}N_3NaO_4S$ [M^+ + Na]: 460.1301, found 460.1282. For aromatized/oxidized signal, HRMS *m/z* calculated for $C_{23}H_{22}N_3O_4S$ [M^+-2+1] 436.1326, found 436.1319.

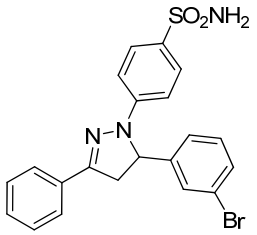

Analog: MLS002699037; CID: 44143703

4-[3-(3-bromophenyl)-5-phenyl-3,4-dihydropyrazol-2-yl] benzene sulfonamide: This analog was prepared as depicted in steps 1 and 2 in Figure 10. Isolated 132mg, 0.29 mmol, 69% yield as a yellow solid. ^{1}H NMR (400 MHz, DMSO-d6) δ 7.79 (dd, *J* = 8.1 Hz, 1.5 Hz, 2H), 7.61 (d, *J* = 9.0 Hz, 2H), 7.52 – 7.39 (m, 5H), 7.31 (t, *J* = 7.8 Hz, 1H), 7.22 (d, *J* = 7.8 Hz, 1H), 7.09 (d, *J* = 8.9 Hz, 2H), 7.04 (s, 2H), 5.68 (dd, *J* = 12.1, 5.1 Hz, 1H), 3.98 (dd, *J* = 17.8, 12.2 Hz, 1H), 3.25 (dd, *J* = 17.8, 5.1 Hz, 1H). ^{13}C NMR (101 MHz, DMSO-d6) δ 149.80, 145.68, 144.31, 133.34, 131.59, 131.39, 130.57, 129.41, 128.72 (x 2), 128.65, 127.23 (x 2), 126.15 (x 2), 124.71, 122.19, 112.01 (x 2), 61.65, 42.79. LCMS retention time: 3.253 min. Parent ion observed as a dimer: HRMS *m/z* calculated for $C_{42}H_{34}Br_2N_6NaO_4S_2$ [$2M^+$ + Na-2]: 933.0325, found 933.0358. For aromatized/oxidized signal, HRMS *m/z* calculated for $C_{21}H_{17}BrN_3O_2S$ [M^+-2+1] 454.0219, found 454.0215.

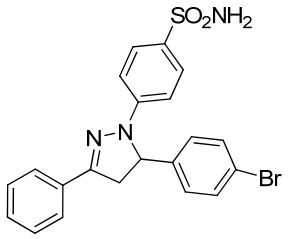

Analog: MLS002699038; CID: 13927312

4-[3-(4-bromophenyl)-5-phenyl-3,4-dihydropyrazol-2-yl]benzene sulfonamide: This analog was prepared as depicted in steps 1 and 2 in Figure 10. Isolated 137mg, 0.30 mmol, 71%) was observed as a white solid. ^{1}H NMR (400 MHz, DMSO-d6) δ 7.79 (dd, *J* = 8.1, 1.5 Hz, 2H), 7.60 (d, *J* = 9.0 Hz, 2H), 7.54 (d, *J* = 8.5 Hz, 2H), 7.44 (m, 3H), 7.22 (d, *J* = 8.5 Hz, 2H), 7.07 (d, *J* = 9.0 Hz, 2H), 7.03 (s, 2H), 5.66 (dd, *J* = 12.1, 5.0 Hz, 1H), 3.97 (dd, *J* = 17.7, 12.1 Hz, 1H), 3.21 (dd, *J* = 17.7, 5.1 Hz, 1H). ^{13}C NMR (101 MHz, DMSO-d6) δ 149.72, 145.69, 140.97, 133.25, 132.00 (x 2), 131.64, 129.38, 128.72 (x 2), 128.12 (x 2), 127.19 (x 2), 126.11 (x 2), 120.66, 112.02 (x 2), 61.69, 42.69. LCMS retention time: 3.269 min. For aromatized/oxidized signal, HRMS *m/z* calculated for $C_{21}H_{17}BrN_3O_2S$ [M^+-2+1] 454.0219, found 454.0221.

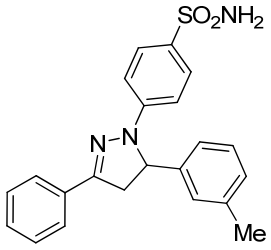

Analog: MLS002699039; CID: 44143700

4-[3-(3-methylphenyl)-5-phenyl-3,4-dihydropyrazol-2-yl] benzene sulfonamide: This analog was prepared as depicted in steps 1 and 2 in Figure 10. Isolated 90mg, 0.23 mmol, 55% yield as a yellow solid. ^{1}H NMR (400 MHz, DMSO-d6) δ 7.79 (dd, *J* = 8.1, 1.5 Hz, 2H), 7.58 (d, *J* = 9.0 Hz, 2H), 7.44 (m, 3H), 7.22 (t, *J* = 7.6 Hz, 1H), 7.14 – 6.97 (m, 7H), 5.58 (dd, *J* = 12.1, 5.4 Hz, 1H), 3.97 (dd, *J* = 17.7, 12.2 Hz, 1H), 3.17 (dd, *J* = 17.7, 5.4 Hz, 1H), 2.26 (s, 3H). ^{13}C NMR (101 MHz, DMSO-d6) δ 149.59, 145.93, 141.75, 138.36, 133.04, 131.76, 129.29, 128.99, 128.72 (x 2), 128.33, 127.13 (x 2), 126.17, 126.07 (x 2), 122.75, 111.93 (x 2), 62.40, 43.04, 21.09. LCMS retention time: 3.212 min. For aromatized/oxidized signal, HRMS *m/z* calculated for $C_{22}H_{20}N_3O_2S$ [M^+-2+1]: 390.1271, found 390.1268.

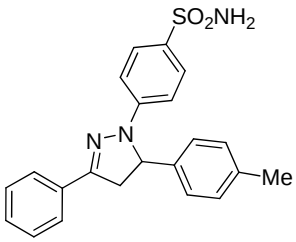

Analog: MLS002699040; CID: 13927310

4-[3-(4-methylphenyl)-5-phenyl-3,4-dihydropyrazol-2-yl] benzene sulfonamide: This analog was prepared as depicted in steps 1 and 2 in Figure 10. Isolated 130mg, 0.33

mmol, 79% yield as a yellow solid. ^{1}H NMR (400 MHz, DMSO-d6) δ 7.79 (dd, *J* = 8.1, 1.5, 2H), 7.58 (d, *J* = 9.0 Hz, 2H), 7.43 (m, 3H), 7.14 (s, 4H), 7.07 (d, *J* = 8.9 Hz, 2H), 7.02 (s, 2H), 5.60 (dd, *J* = 12.1, 5.1 Hz, 1H), 3.95 (dd, *J* = 17.7, 12.1 Hz, 1H), 3.16 (dd, *J* = 17.7, 5.1 Hz, 1H), 2.24 (s, 3H). ^{13}C NMR (101 MHz, DMSO-d6) δ 149.60, 145.86, 138.64, 136.81, 132.99, 131.80, 129.63 (x 2), 129.27, 128.71 (x 2), 127.09 (x 2), 126.04 (x 2), 125.68 (x 2), 112.00 (x 2), 62.14, 42.94, 20.62. LCMS retention time*:* 3.224 min. For aromatized/oxidized signal, HRMS *m/z* calculated for $C_{22}H_{20}N_3O_2S$ [M^+-2+1] 390.1271, found 390.1266.

i. SUMMARY OF PROBE PROPERTIES: MLS002699035; CID: 2950007

Physical appearance and properties: The compound was isolated as white needles with melting point range of 185-187 °C. The compound formed a mass when collected as described above that resembled spun wool. The purity was determined to be 97% by LCMS at 254 nm.

LCMS behavior: Upon analysis by LCMS, compounds of this type commonly showed a mass consistent with aromatization/oxidation of the central dihydropyrazoline core, [M^+-2+1]. This was determined to be an artifact of the LCMS method, as the ratio of parent ion [M^+ + 1] to oxidized ion [M^+-2+1] could be modulated to a limited degree by varying the method parameters. Additionally, compounds that showed significant ratios of the two ions by LCMS were clearly pure by ^{1}H NMR and were not mixtures reflective of the observed LCMS product ratio.

It is also notable that intentionally prepared oxidized analogs were compared to their unoxidized dihydropyrazoline analogs by ^{1}H NMR and by bioassay. The oxidized compounds were easily recognized by diagnostic signals in the ^{1}H NMR and did not possess GTPase inhibitory activity.

^{1}H and ^{13}C NMR in $CDCl_3$: The probe compound NMR characterization was obtained in DMSO-d6 and $CDCl_3$. The DMSO data can be directly compared to the other analogs and is represented in the experimental section. The $CDCl_3$ data is offered here for convenience.

^{1}H NMR (400 MHz, $CDCl_3$) δ 7.73 (m, 2H), 7.67 (d, *J* = 9.0 Hz, 2H), 7.39 (m, 3H), 7.15 (d, *J* = 8.7 Hz, 2H), 7.07 (d, *J* = 8.9 Hz, 2H), 6.84 (d, *J* = 8.7 Hz, 2H), 5.31 (dd, *J* = 12.1, 5.8 Hz, 1H), 4.60 (s, 2H), 3.85 (dd, *J* = 17.3, 12.1 Hz, 1H), 3.76 (s, 3H), 3.18 (dd, *J* = 17.3, 5.8 Hz, 1H). ^{13}C NMR (101 MHz, $CDCl_3$) δ 159.55, 149.75, 147.59, 133.43, 132.24, 130.43, 129.66, 128.91 (x 2), 128.25 (x 2), 127.09 (x 2), 126.33 (x 2), 114.98 (x 2), 112.82 (x 2), 63.32, 55.53, 43.92.

Literature precedent of synthesis and melting point: The synthesis and melting point of this compound has been described (Faid-Allah, 1988). The literature melting point was reported as 216 °C which was higher than that which was experimentally determined in our lab (mp 185-187 °C). We cannot account for the discrepancy, but we noted it.

j. TABULATED SUMMARY OF KNOWN PROBE PROPERTIES: See page 1

4. Comparison to Prior Art for Cdc42 Inhibitors

As stated in the CPDP for this project there was no prior art describing direct Cdc42 inhibitors, so the discoveries reported here are highly innovative and impactful. Shown below is the structure of Secramine which is not a direct inhibitor of Cdc42. The compound

was synthesized predicated on brefeldin A, which is a fungal metabolite. that stabilizes a complex between Arf and Arf GEF thereby blocking GTPase activation (Pelish 2006).

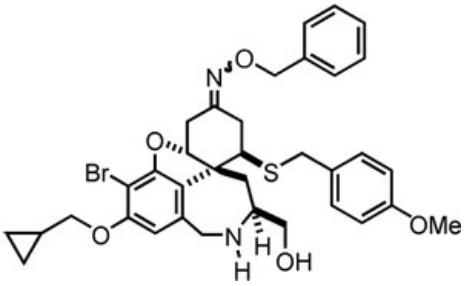

Secramine

The stability, solubility and broad-spectrum target profiling of these compounds has yet to be assessed. With respect to stability, deterioration of compound purity was not observed over weeks during which time the compounds were handled. Spontaneous oxidation of the central pyrazoline core was also not observed unless under the conditions of LCMS analysis. Moreover, with respect to solubility and cross-target reactivity, this structural class of compounds has been dosed orally and shown to inhibit COX-1 and COX-2 enzymes in a rat carrageenan model of inflammation (Rathish, 2009). Modified versions of the structural class, of which Celecoxib belongs, have been pursued clinically and shown to be therapeutically useful oral agents.

5. Bibliography

Agarwal V, Hammerschmidt S. Cdc42 and the phosphatidylinositol 3-kinase-Akt pathway are essential for PspC-mediated internalization of pneumococci by respiratory epithelial cells. J Biol Chem. 2009;284:19427-36.

Boettner B, Van Aelst L. The role of Rho GTPases in disease development. Gene. 2002 20;286(2):155-74

Bos JL, Rehmann H, Wittinghofer A. GEFs and GAPs: critical elements in the control of small G proteins. Cell. 2007;129(5):865-77.

Chang YW, Bean RR, Jakobi R. Targeting RhoA/Rho kinase and p21-activated kinase signaling to prevent cancer development and progression. Recent Pat Anticancer Drug Discov. 2009;4:110-24

Chimini G, Chavrier P. Function of Rho family proteins in actin dynamics during phagocytosis and engulfment. Nat Cell Biol. 2000; 2: E191-6.

Dutra JM, Bonilha VL, De Souza W, Carvalho TM. Role of small GTPases in Trypanosoma cruzi invasion in MDCK cell lines. Parasitol Res. 2005;96:171-7.

Etienne-Manneville S, Hall A: Rho GTPases in cell biology. Nature 2002; 420:629-635

Faid-Allah, HM; Mokhtar, HM. Pyrazole derivatives with possible hypoglycemic activity. Indian Journal of Chemistry, Section B: Organic Chemistry Including Medicinal Chemistry 1988; 27B: 245-249.

Gao Y, Dickerson JB, Guo F, Zheng J, Zheng Y. Rational design and characterization of a Rac GTPase-specific small molecule inhibitor. Proc Natl Acad Sci 2004 May 18;101(20):7618-23.

Gómez del Pulgar T, Benitah SA, Valerón PF, Espina C, Lacal JC. Rho GTPase expression in tumorigenesis: evidence for a significant link. Bioessays. 2005;27:602-13.

He B, Chen P, Chen SY, Vancura KL, Michaelis S, Powers S. RAM2, an essential gene of yeast, and RAM1 encode the two polypeptide components of the farnesyltransferase that prenylates a-factor and Ras proteins. Proc Natl Acad Sci U S A. 1991, 88:11373-7.

Isleyen, A; Dogan, O. Application of ferrocenyl substituted aziridinylmethanols (FAM) as chiral ligands in enantioselective conjugate addition of diethylzinc to enones. Tetrahedron: Asymmetry. 2007:18: 679-684.

Jaffe AB, Hall A: Rho GTPases: biochemistry and biology. Annu Rev Cell Dev Biol 2005; 21:247-269.

Johnson JL, Erickson JW, Cerione RA. New insights into how the Rho guanine nucleotide dissociation inhibitor regulates the interaction of Cdc42 with membranes. J. Biol. Chem. 2009; 284:23860-71.

Kozma R, Ahmed S, Best A, Lim L. The Ras-related protein Cdc42Hs and bradykinin promote formation of peripheral actin microspikes and filopodia in Swiss 3T3 fibroblasts. Mol Cell Biol. 1995;15:1942-52.

Kuckuck FW, Edwards BS, Sklar LA. High throughput flow cytometry. Cytometry. 2001;44:83-90.

Pelish HE, Peterson JR, Salvarezza SB, Rodriguez-Boulan E, Chen JL, Stamnes M, Macia E, Feng Y, Shair MD, Kirchhausen T. Secramine inhibits Cdc42-dependent functions in cells and Cdc42 activation in vitro. Nat Chem Biol. 2006 ;2:39-46.

Penning, TD; Talley, JJ; Bertenshaw, SR; Carter, JS; Collins, PW; Docter, S; Graneto, MJ; Lee, LF; Malecha, JW; Miyashiro, JM; Rogers, RS; Rogier, DJ; Yu, SS; Anderson, GD; Burton, EG.; Cogburn, JN; Gregory, SA; Koboldt, CM; Perkins, WE; Seibert, K; Veenhuizen, AW; Zhang, YY; Isakson, PC. Synthesis and Biological Evaluation of the 1,5-Diarylpyrazole Class of Cyclooxygenase-2 Inhibitors: Identification of 4-[5-(4-Methylphenyl)-3-(trifluoromethyl)-1H-pyrazol-1-yl]benzenesulfonamide (SC-58635, Celecoxib). J. Med. Chem. 1997: 40: 1347-1365

Raftopoulou M, Hall A. Cell migration: Rho GTPases lead the way. Dev Biol. 2004;265:23-32

Rathish IG, Javed K, Ahmad S, Bano S, Alam MS, Pillai KK, ,Singh S, Bagchi V. Synthesis and antiinflammatory activity of some new 1,3,5-trisubstituted pyrazolines bearing benzene sulfonamide. Bioorg. Med. Chem. Lett. 2009, 19, 255-258

Ridley AJ. Rho GTPases and actin dynamics in membrane protrusions and vesicle trafficking. Trends Cell Biol. 2006

Rossman KL, Der CJ, Sondek J. GEF means go: turning on RHO GTPases with guanine nucleotide-exchange factors. Nat Rev Mol Cell Biol. 2005;6:167-80

Sahai E, Marshall CJ. RHO-GTPases and cancer. Nat Rev Cancer. 2002;2:133-42.

Schwartz SL, Tessema M, Buranda T, Pylypenko O, Rak A, Simons PC, Surviladze Z, Sklar LA, Wandinger-Ness A. Flow cytometry for real-time measurement of guanine nucleotide binding and exchange by Ras-like GTPases. Anal Biochem. 2008;381:258-66.

Shutes A, Onesto C, Picard V, Leblond B, Schweighoffer F, Der CJ. Specificity and mechanism of action of EHT1864, a novel small molecule inhibitor of Rac family small GTPases. J. Biol. Chem. 2007;282:35666-78.

Surviladze Z, Dráberová L, Kubínová L, Dráber P. Functional heterogeneity of Thy-1 membrane microdomains in rat basophilic leukemia cells. Eur J Immunol. 1998;28:1847-58.

Surviladze Z, Waller A, Wu Y, Romero E, Edwards BS, Wandinger-Ness A, Sklar LA. Identification of a small GTPase inhibitor using a high-throughput flow cytometry bead-based multiplex assay. J. Biomol. Screen. 2010;15:10-20.

Takai Y, Sasaki T, Matozaki T. Small GTP-binding proteins. Physiol Rev. 2001;81:153-208.

Van den Broeke C, Radu M, Chernoff J, Favoreel HW. An emerging role for p21-activated kinases (Paks) in viral infections. Trends Cell Biol. 2010 Jan 11. [Epub ahead of print]

Van Hennik PB, Hordijk PL. Rho GTPases in hematopoietic cells. Antioxid Redox Signal. 2005;7:1440-55.

Vega FM, Ridley AJ. Rho GTPases in cancer cell biology. FEBS Lett. 2008; 582:2093-101

Wilson BS, Seagrave J, Oliver JM. Impaired secretion and increased insolubilization of IgE-receptor complexes in mycophenolic acid-treated (guanine nucleotide-depleted) RBL-2H3 mast cells. J Cell Physiol. 1991;149:403-7

Yang L, Wang L, Zheng Y. Gene targeting of Cdc42 and Cdc42GAP affirms the critical involvement of Cdc42 in filopodia induction, directed migration, and proliferation in primary mouse embryonic fibroblasts. Mol Biol Cell. 2006; 17:4675-85.

Zhang B, Zhang Y, Shacter E, Zheng Y. Mechanism of the guanine nucleotide exchange reaction of Ras GTPase--evidence for a GTP/GDP displacement model. Biochemistry. 2005; 44:2566-76.